^{13}C n.m.r. study of phase heterogeneity in poly(phenylene sulphide)

Peter Pengtao Huo and Peggy Cebe*

Department of Materials Science and Engineering, Massachusetts Institute of Technology, Cambridge, MA 02139, USA

Solid state ^{13}C n.m.r. was used to study the phase heterogeneity of poly(phenylene sulphide), PPS, at room temperature. Relative fractions of crystal, rigid amorphous and liquid-like amorphous phases were determined from X-ray and thermal analyses. Samples containing very different fractions were examined using cross-polarization contact time and spin-lattice relaxation measurements. The optimum carbon/proton contact time for cross-polarization/magic angle spinning studies was found to be $\sim 1000\,\mu s$. Peak intensity of the protonated carbons was studied as a function of delay time. A pronounced amorphous halo exists in the n.m.r. spectrum of PPS films containing a large fraction of liquid-like amorphous phase, and the halo decreases significantly with increasing delay time. A very insignificant halo exists in the n.m.r. spectrum of PPS containing a large fraction of rigid amorphous phase. We conclude that this halo is from the most mobile, liquid-like amorphous phase. Using spin-lattice relaxation measurements, we studied the dynamic heterogeneous phase behaviour of PPS. Here we find that from the standpoint of spin-lattice relaxation time, T_1, 100% amorphous PPS shows phase heterogeneity at room temperature. The longest T_1 is $\sim 45\,s$, corresponding to a mass fraction of 0.57. In semicrystalline PPS, spin-lattice relaxation measurements show a much larger amount of the material possesses longer relaxation time. The T_1 of semicrystalline PPS ranges from 150 to 200 s, corresponding to mass fractions of 0.91–0.94. This indicates that semicrystalline PPS is more nearly homogeneous: the crystals and most of the amorphous phase are very 'rigid' at temperatures far below the glass transition of PPS.

(Keywords: ^{13}C n.m.r.; phase heterogeneity; poly(phenylene sulphide))

INTRODUCTION

Many semicrystalline engineering thermoplastics have a non-crystalline phase which is heterogeneous, that is, the non-crystalline material may contain regions which exhibit distinctly different properties. Dielectric relaxation[1-3], thermal analysis[4-9], n.m.r.[10-12] and transport properties[13] have all been used to examine the amorphous phase heterogeneity. We have recently studied the composite matrix polymer poly(phenylene sulphide), PPS, using dielectric and thermal analysis[1,4]. Based on measurements of heat capacity increment at the glass transition temperature, T_g, the amorphous phase of PPS was identified to consist of chains of greater and lesser mobility, which were termed the liquid-like amorphous phase and the rigid amorphous phase (RAP), respectively[1]. The liquid-like amorphous phase has a distinct step in heat capacity at its T_g, while the RAP does not.

We subsequently showed that, as a consequence of our new heat of fusion of PPS[4], the amount of RAP in PPS may be as large as 0.42 by weight depending upon thermal treatment. We also showed that dielectric relaxation intensity is a very sensitive indicator of the molecular mobility of RAP near the glass transition of the mobile amorphous phase[1]. RAP material makes no contribution to dielectric relaxation below the T_g, but RAP relaxes little by little in the temperature range between T_g and

the crystal melting point[1]. Therefore, RAP does not display its own separate T_g in PPS. In spite of the very large weight fraction of RAP material, from either thermal analysis or dielectric relaxation there is no sign of any difference at room temperature between the properties of the liquid-like amorphous phase and the RAP.

From the above experiments, the amorphous phase of PPS appears homogeneous at room temperature. However, other experiments have shown differences in the nature of the amorphous phase even far below the T_g for a related engineering thermoplastic polymer poly(ether ether ketone), PEEK. Recently, Michele and Vittoria[13] used diffusion measurements to study the phase heterogeneity of PEEK. This polymer, like PPS, exhibits a large RAP fraction, as measured by dielectric relaxation[3] and heat capacity[4]. These authors found that at room temperature the diffusion coefficient of the RAP is different from that of the liquid-like amorphous phase, and is the same as that of the crystal phase[13].

To study the different behaviours of the crystal and amorphous phases of PPS at room temperature, we selected a different probe that is sensitive to small scale structural variations. Here, we report our high resolution cross-polarization/magic angle spinning (CP/MAS) ^{13}C solid state n.m.r. study of amorphous and semicrystalline PPS at room temperature. We find that even at room temperature, the amorphous phase in semicrystalline PPS shows heterogeneity. For PPS containing both RAP

---

and a large fraction of liquid-like amorphous phase, the liquid-like amorphous phase at room temperature shows a different chemical shift from that of the RAP.

EXPERIMENTAL

Material characterization

Semicrystalline Ryton V-I grade PPS films (75 μm thick) were provided by Phillips Petroleum. An amorphous sample was made by heating the as-received film to 320°C, holding for 2 min, and then quenching in cold water. An isothermally cold crystallized sample was prepared by heating the quenched amorphous film from room temperature to 170°C in a Mettler FP80 hot stage and holding for 30 min in an inert gas environment. Crystallization kinetics and melting behaviour of these samples have been reported in our previous studies[14-16].

Relative fractions of crystal, liquid-like amorphous and rigid amorphous phases, density and thermal properties are listed in *Table 1* for quenched amorphous PPS, as-received film and film cold crystallized at 170°C. Degree of crystallinity was determined from density, area under the d.s.c. endotherm, and area under the wide angle X-ray scattering curve[1,4]. All these measurements indicated that the quenched PPS sample is completely amorphous. In addition, the as-received film and that cold crystallized at 170°C have nearly the same degree of crystallinity (0.37 and 0.34, respectively), and hence about the same *total fraction* of non-crystalline material. Note, however, from *Table 1* that these two samples have very different amounts of RAP, which is deduced both from dielectric analysis[1] and from the heat capacity increment at the glass transition of the liquid-like amorphous phase[1-9]. The liquid-like amorphous phase is defined as the portion of the amorphous phase that contributes to the glass transition heat capacity step, and is in random-coil-like morphology with relatively high mobility[1,3,4]. The RAP, on the other hand, does not contribute to the heat capacity step at T_g, and it has an intermediate morphology between the liquid-like or random-coil-like amorphous phase, and shows less mobile behaviour. In the sample cold crystallized at 170°C the RAP fraction is 0.36. In the as-received sample the RAP fraction is 0.63 which in fact is all of the non-crystalline material, since for this material there is no liquid-like amorphous phase. Therefore, the major

difference between the two semicrystalline PPS materials is the nature of the amorphous phase.

Two methods were used to examine the glass transition region. The T_gs in *Table 1* were determined calorimetrically using the midpoint in the heat capacity step obtained from the d.s.c. scan at 20°C min^{-1}. The as-received sample showed no heat capacity step and we were unable to determine its T_g by calorimetry. Dielectric relaxation was the second method used to determine T_g, from the peak position of the loss maximum at a frequency of 1.0 kHz over the temperature range from room temperature up to 180°C[1]. The as-received film has a dielectric loss that is shifted to higher temperature, and is broader with much weaker intensity than that of the cold crystallized material[1].

Solid-state n.m.r.

Solid-state [13]C n.m.r. spectra were obtained using an IBM NR/200 AF (4.7 T) spectrometer operating at 50.3 MHz fitted with an IBM Solid Accessory Rack which housed the high-power amplifier, and Doty Scientific probe for magic angle spinning. Dipolar decoupling was used in conjunction with a cross-polarization pulse sequence employing a 5 μs proton 90° pulse and a 3 s recycle delay time. Solid-state spectra were referenced to the methyl resonance of p-di-tert-butylbenzene (31.0 ppm from TMS).

Relaxation studies were conducted with modified Torchia's pulse sequence[17] in which ^{13}C magnetization is initially polarized via the protons into the plane perpendicular to the external magnetic field, H_0. Following this cross-polarization, a 90° pulse places the ^{13}C magnetization into the -z direction with respect to H_0 so that relaxation occurs under the influence of this external field. After fixed delay times ranging from 0 to 30 s, the magnetization was flipped back into the xy plane for signal detection. For each delay time, 2048 transients were collected and Fourier transformed with intensities scaled to the free induction decay for delay time equal to zero. Peak intensities were plotted as a function of delay time and analysed at long times for the straight-line portion of the curve according to the following equation:

$$\ln M(t) = \ln C - t/T_1 \qquad (1)$$

where $M(t)$ is the peak intensity as a function of delay time, T_1 is the spin-lattice relaxation time and C is a constant related to the mass fraction of the component with relaxation time T_1. A least-squares fitting of the straight-line portion of the relaxation curves yielded the values of C from the y-intercept and T_1 from the inverse slope.

Table 1 Crystalline, amorphous and rigid amorphous phase fractions, density, glass transition temperatures and melting peak temperatures of PPS

PPS sample	Quenched	As-received	Cold crystallized at 170°C
χ_c	0	0.37	0.34
χ_a	1	0	0.30
$\chi_{RAP}(=1-\chi_c-\chi_a)$	0	0.63	0.36
ρ(g cm^{-3})	1.3195	1.3571	1.3533
T_g(°C)^a	92	–^{c}	107
T_g(°C)^b	111	133	125
T_{m1}(°C)	–^{c}	261	187
T_{m2}(°C)	278	280	277

^{a} Measured by using d.s.c. at a scan rate of 20°C min^{-1}
^{b} Measured by using dielectric loss maximum at 1000 Hz
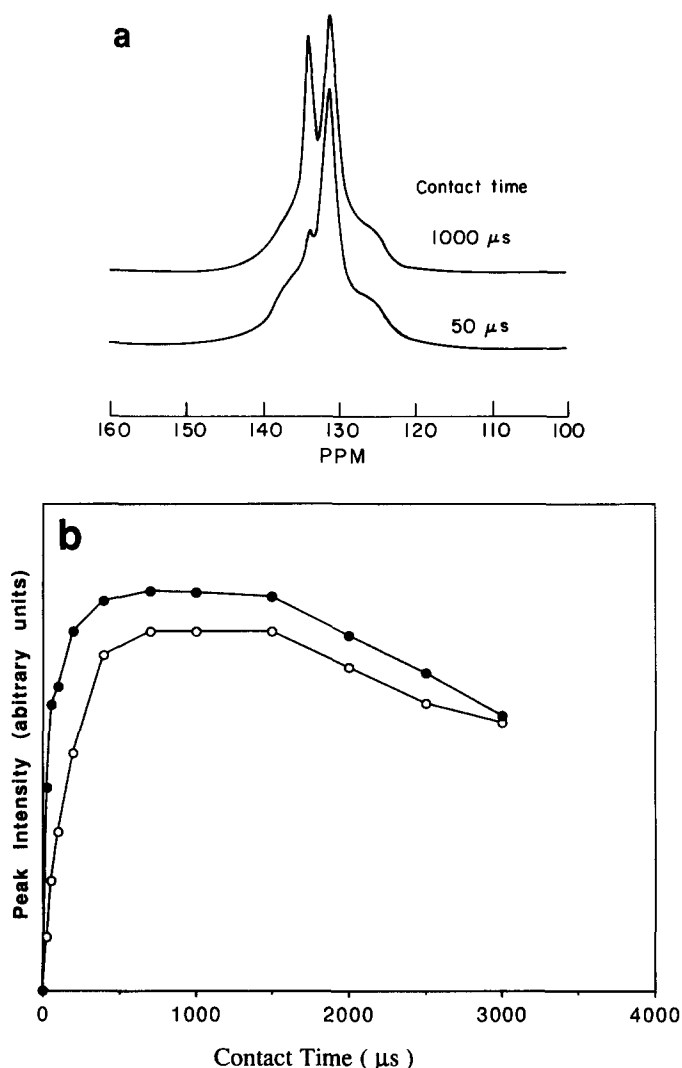^{c} None observed

RESULTS AND DISCUSSION

Here we show for the first time the dependence of the peak intensity *versus* cross-polarization contact time for PPS semicrystalline as-received film. For the cross-polarization technique, the contact time is crucial because of differences in efficiency of coupling ^{13}C and ^{1}H magnetization for the protonated and non-protonated carbons. In fact, contact time dependence studies provide another way to assign the peaks to protonated or non-protonated carbons. We present in *Figure 1a* the cross-polarization contact time dependence of PPS as-received semicrystalline sample, for two different contact times of 50 and 1000 μs. At a contact time of

nuclei have very efficient coupling to ^{1}H proton polarization. At intermediate contact time, from 700 to 1500 μs, both protonated and non-protonated carbon peaks reach their maximum intensity. At contact times of >1500 μs both peak intensities decrease, since now relaxation of protons takes place and shows significant effect on the carbons at these longer contact times.

Now the contact time is fixed at 1000 μs, and the delay time is varied. *Figure 2* shows the n.m.r. spectra for the amorphous film, as-received semicrystalline film and film cold crystallized at 170°C at two different delay times (0 and 30 s). The ^{13}C CP/MAS spectrum for the amorphous sample (*Figure 2a*) shows two poorly resolved broad peaks ranging from 120 to 140 ppm, 20 ppm wide at half maximum, similar to that reported previously[18–20].
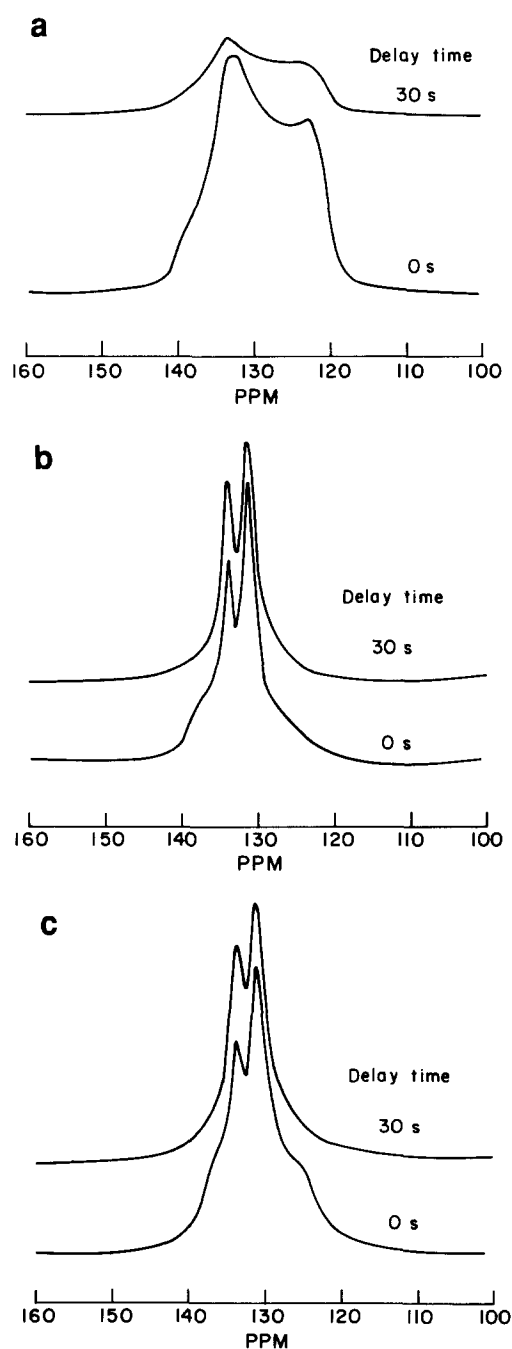
Figure 1 (a) CP/MAS ^{13}C solid state n.m.r. spectra of as-received PPS film, at cross-polarization contact times of 50 μs and 1000 μs. (b) Peak intensity *versus* cross-polarization contact time of protonated (●) and non-protonated (○) carbons for as-received PPS film

Figure 2 CP/MAS ^{13}C solid state n.m.r. spectra at the delay times indicated, for PPS film: (a) quenched amorphous; (b) as-received; (c) cold crystallized at 170°C

50 μs, we observe a shoulder at 126 ppm, a strong peak at 131 ppm and a very small peak at 134 ppm. The two sharp peaks are due to the two distinct carbons in the crystal phase of semicrystalline PPS. These peaks do not appear in the spectrum of quenched 100% amorphous PPS. The assignment of these two peaks has been made previously[18–20]: the peak at 131 ppm is due to protonated carbons, while the 134 ppm peak is due to the non-protonated carbons. At a contact time of 1000 μs, the protonated and the non-protonated carbon peaks are comparable in intensity. In *Figure 1b*, the peak intensity is presented as a function of contact time for both protonated and non-protonated carbons. At short contact time (e.g. <100 μs), the non-protonated carbon peak is still very weak, while the protonated carbon peak reaches a higher intensity. For the non-protonated carbon, there is no efficient route to exchange magnetization between the ^{13}C and ^{1}H nuclei due to the lack of ^{1}H within nearest neighbour distances. Therefore in the cross-polarization experiment, a longer contact time is required for magnetization to build up for the non-protonated carbon than for the protonated carbon. For the protonated carbons, only a very short contact time is needed to build up magnetization since these
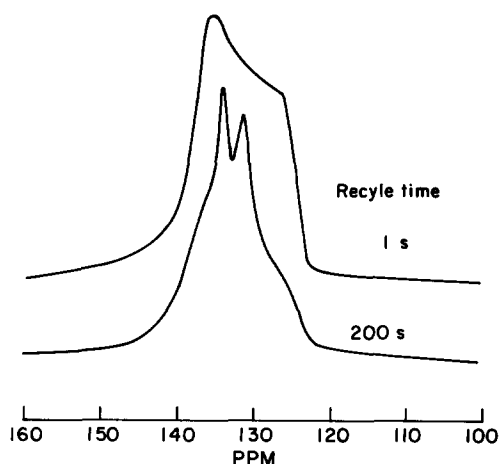
Figure 3 Direct polarization/magic angle spinning ^{13}C solid state n.m.r. spectra for PPS as-received film at recycle times of 1 and 200 s

The intensity of the amorphous peaks decreases greatly as the delay time increases from 0 to 30 s, but the peak line shape remains the same. At a delay time of 30 s, the intensity is only one-quarter to one-third of the intensity at zero delay time, which has been shown in *Figure 2a*, which reflects the spin-lattice relaxation of spins in the quenched 100% amorphous sample. For both the as-received film and PPS cold crystallized at 170°C, *Figures 2b* and *c*, respectively, we observe two very sharp, well resolved peaks located at 131 and 134 ppm, for both 0 and 30 s delay times. Furthermore, in spite of the fact that the degree of crystallinity is very nearly the same, the as-received sample has relatively sharper peaks than that cold crystallized at 170°C. The full widths at half maximum (FWHM) for the as-received and cold crystallized samples are 4.4 and 6.2 ppm, respectively. In previous study of PPS, Clark et al.[18] assumed that the FWHM scaled with degree of crystallinity between two known extrema, and from measured FWHM deduced intermediate degrees of crystallinity. A sample with a FWHM of 8.9 ppm was deduced to have a crystallinity of 0.36, which is comparable to our PPS samples. We have recently calculated the heat of fusion of PPS and shown that the degrees of crystallinity of commercial material are much smaller than previously believed[4]. Thus, the extreme value of 65% crystallinity used by Clark et al.[18] is most likely incorrect. From the present work we see that for samples with nearly the same degree of crystallinity, very different FWHM are observed, depending upon degree of crystal perfection and amount of RAP. The assumption of a linear relation between FWHM and crystallinity is not borne out.

Beside the sharp peaks which come from the crystal phase, one can observe a broad halo underneath the two peaks, which is due to the amorphous phase in the semicrystalline PPS samples[18–20]. Compared with the as-received sample at zero delay time (the usual CP/MAS n.m.r. spectrum), we found that the sample cold crystallized at 170°C (*Figure 2c*) has a much more distinct amorphous halo underneath the crystalline peaks. For this sample, we observe a small broad peak at ∼128 ppm and a large shoulder at 140 ppm which are located at about the same chemical shift as the broad peaks in the spectrum of the quenched 100% amorphous sample. For the as-received sample (*Figure 2b*), the halo is much less distinct: the peak at 128 ppm is absent and the shoulder at 140 ppm is much smaller.

In the PPS cold crystallized at 170°C, we also observed that the amorphous halo intensity decreases dramatically with the delay time, in a manner similar to the quenched 100% amorphous sample, which implies again that this broad shoulder is due to the mobile amorphous phase in the semicrystalline sample. The halo underneath the as-received sample also decreases in intensity with an increase in delay time, but the effect is not as noticeable because the intensity of the halo at 0 s delay time is not very large in this sample. Therefore, for both semicrystalline samples, the whole line width decreases with increasing delay time, and this is especially apparent for the cold crystallized sample. We realize something different in the amorphous phase behaviour for the as-received sample compared to the sample cold crystallized at 170°C. As listed in *Table 1*, the crystallinities of the as-received film and the sample cold crystallized at 170°C are 0.37 and 0.34, respectively. The total amorphous fraction, $1 - \chi_c$, for these two semicrystalline samples is nearly the same. But, there is a great difference in the amount of liquid-like amorphous phase material. The cold crystallized sample has $\chi_a = 0.30$ while the as-received sample has no liquid-like amorphous phase ($\chi_a = 0$ by thermal analysis[1]). Therefore, the differences in the observed halo can be explained on the basis of the different amorphous phase rigidity. The halo in the semicrystalline samples reflects a portion of the amorphous phase which has a random-coil-like morphology, with mobility similar to the amorphous phase in the quenched 100% amorphous PPS material. The rigid nature of the amorphous phase material in the as-received film makes this sample have a much smaller halo, less subject to relaxation. By either dielectric or heat capacity measurements[1,4] this as-received film had no liquid-like amorphous phase.

From thermal analysis, the liquid-like amorphous phase in semicrystalline samples behaves very much like the amorphous phase in the quenched PPS sample, that is, it shows a distinct heat capacity increment at T_g. It is the portion of the amorphous phase that has random-coil like morphology, and is thought to be located in regions of decreased chain constraint, for example, farther from the crystal fold surfaces in regions large enough for co-operative rearrangements to occur[4]. We therefore can expect the contribution of the liquid-like amorphous phase inside the semicrystalline sample to be very similar to that of the quenched 100% amorphous PPS shown in *Figure 2a*. From *Figure 2a*, we find that the liquid-like amorphous phase material has a very different, very broad line shape compared with the two sharp peaks seen in semicrystalline PPS. The RAP, on the other hand, represents material of reduced molecular mobility possibly the result of an increase in chain constraints. For example, the RAP material may be located in the crystal/amorphous interphase where it may be highly entangled with the crystals[1,3,4], or in regions that are too small to allow the type of co-operative rearrangements necessary to exhibit a heat capacity step at T_g[4]. It is then reasonable to say that RAP has a morphology intermediate between that of the crystal and the liquid-like amorphous phase. RAP, which shows more order than the random coil but less order than the crystals, should have the n.m.r. resonant line width narrower than liquid-like amorphous phase but wider than the crystal peaks. By comparing the line shape for the as-received sample and cold crystallized sample, we conclude that

RAP cannot have a line width as wide as that of the liquid-like amorphous phase, otherwise both as-received sample and cold crystallized sample should have almost identical line shapes.

To verify that only liquid-like amorphous phase having random-coil-like morphology contributes to the amorphous halo in *Figures 2b* and *c*, we performed a *direct polarization* study for the semicrystalline, as-received sample using different recycle times. Here, we took advantage of the very different relaxation time of the liquid-like amorphous phase compared to that of either RAP or the crystals. *Figure 3* shows the results for recycle times of 1 and 200 s. The spectrum of 1 s recycle time has been greatly magnified in *Figure 3*, being increased by about a factor of 20 compared to the spectrum at 200 s recycle time. For 1 s recycle time, only that portion of material with relaxation time shorter than 1 s can contribute to the spectrum, while other portions of material with longer relaxation times are suppressed. We first observe a broad resonant peak with chemical shift ranging from 120 to 140 ppm, very similar to the quenched 100% amorphous phase shown in *Figure 2a*. This portion of material with relaxation time of <1 s is only from the liquid-like amorphous phase. Note that the rigid amorphous and crystal phases have a relaxation time much longer than 1 s, and therefore are suppressed when 1 s repeating time was used. When the repeating time is increased to 200 s, we observed both amorphous halo and emergence of the crystal peaks at 131 and 134 ppm, an indication of the crystal phase spectrum. Since 200 s is comparable to, if not longer than, the crystal relaxation time, we observed both crystal and amorphous phase components in the spectrum. Again note the different scale for the two different recycle times in *Figure 3*. The absolute intensity for delay time 1 s is very low, only about one-twentieth that of delay time 200 s, implying that there exists only a tiny amount of liquid-like amorphous in as-received sample, which accounts for the small, indistinct halo in *Figure 2b*.

This very small amount of liquid-like amorphous phase for the as-received sample was not able to be detected either by d.s.c. or by dielectric spectroscopy[1,4]. As described previously, at room temperature (which is far below the T_g of PPS) we saw no difference between the liquid-like amorphous phase and RAP either by thermal analysis[4] or by dielectric relaxation[1]. The calculation of the relative amounts of liquid-like amorphous phase is based on the contribution made to the heat capacity increment at the T_g, which is a much higher temperature than the present room temperature study[1-9]. In fact, at temperatures far below T_g, the heat capacity of crystal and amorphous phases are the same[4], irrespective of the degree of order. The heat capacity, in this sense, is insensitive to the order or local environment at low temperature in the samples. However, n.m.r. as indicated above, is very sensitive to the local environment of the spins. The chemical shift is directly related to the local magnetic field. The spins in the well ordered crystal phase, in the very random coil-like (more mobile) amorphous phase, or in the intermediate (less mobile) RAP feel a different local environment. This difference in molecular arrangement or local environment leads to a different local magnetic field for the spins, resulting in different chemical shifts and therefore line shapes.

From the qualitative line shape study, we have detected phase heterogeneity among crystal phase, liquid-like
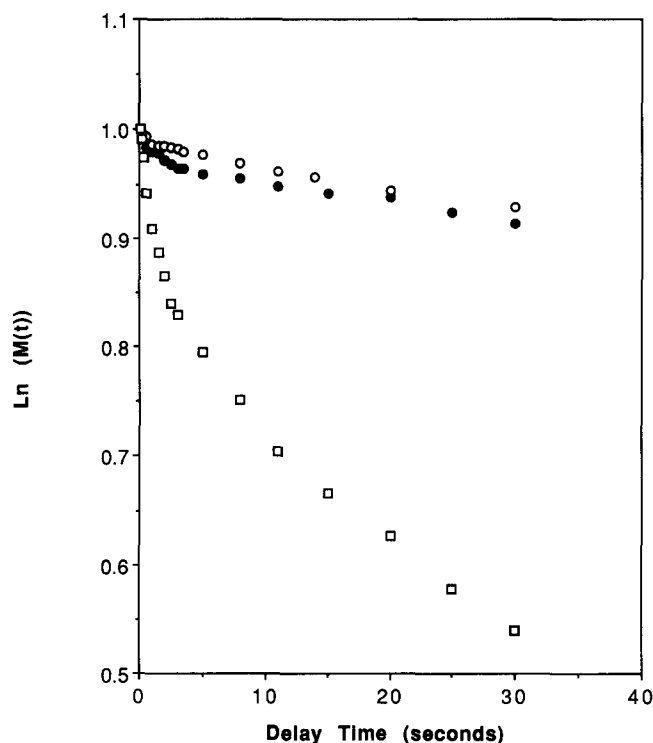

Figure 4 Ln(magnetization), ln $M(t)$, *versus* delay time for PPS film: quenched amorphous ($\square$); as-received ($\bigcirc$); cold crystallized at 170°C ($\bullet$)

Table 2 Protonated carbon spin-lattice relaxation times and mass fractions of PPS

Sample	Relaxation time (s)[a]		Mass fraction[a]	
	T_{1S}	T_{1F}	M_S	M_F
Quenched amorphous	45	–[b]	0.57	–[b]
As-received	152	0.57	0.94	0.06
Cold crystallized at 170°C	198	0.56	0.91	0.09

[a] S and F refer to slow and fast components, respectively
[b] None calculated

amorphous phase and RAP, even at a temperature far below the T_g of PPS. Thereafter, we used spin-lattice relaxation experiments to study the *dynamic* heterogeneous phase behaviour. *Figure 4* shows plots of ln(magnetization) *versus* delay time. The plots are curves rather than straight lines, indicating clearly that at room temperature there exists dynamic heterogeneity in both purely amorphous and semicrystalline PPS. However, in spite of curvature at low values of delay time, there is part of the curve which may be approximated by a straight line at longer values of delay time. This portion of the curve was used to determine T_1. The T_1 values and mass fraction of the component relaxing with characteristic time T_1 are listed in *Table 2* for all samples.

The T_1 for the amorphous sample was determined by using the maximum value of magnetization at a chemical shift of 140 ppm. In fact, the line *shape* of quenched 100% amorphous PPS remains almost the same regardless of delay time. We found that a single exponential was not sufficient to characterize the quenched amorphous relaxation curve, and we therefore only analysed the component that relaxes the slowest, i.e. having longest T_1, and computed its corresponding mass fraction. The

longest T_1 is ~ 45 s, corresponding to mass fraction of 0.57. The dispersion of the T_1 delay curve suggests that there exists a dynamic heterogeneity in the purely amorphous sample at temperatures far below the T_g. In other words, even purely amorphous material which is all in random-coil-like morphology, will exhibit some distribution in the relaxation time.

For the semicrystalline samples, we only analyse T_1 for the protonated carbon with chemical shift of 131 ppm, since T_1 for the non-protonated carbons was extremely long. (We see no decay in the non-protonated peak intensity compared to that of protonated carbons.) The dispersion curves for both as-received and cold crystallized samples can be fitted using two exponential decays, indicating the existence of two species of material in the sense of dynamic mobility. We call the two species the slow and fast portion according to their T_1 values. The T_1 values of the slow portion of as-received and cold crystallized samples are 152 and 198 s, respectively. Besides the slow portion, we have also calculated the T_1 of the fast portion (steeply decreasing part of the curve in *Figure 4*) which shows T_1 of <1 s for both as-received and cold crystallized samples.

The values of the longest relaxation times for the protonated carbons are only about one-third of the T_1 results reported by Gomez and Tonelli[20] for semicrystalline PPS. These authors report a relaxation time of 486 s for protonated carbons, and additionally, they report that the relaxation time of the non-protonated carbons is nearly the same at 532 s. Thus, according to these authors there was no significant difference in the ability of the non-protonated carbons to relax compared to the carbons with proton nearest neighbours. On the other hand in this work we find that the T_1 for non-protonated carbons is at least five times longer compared with those of protonated carbons listed in *Table 2*. This seems reasonable since the non-protonated carbons lack an efficient relaxation mechanism. Also, the empirical rule that the product of T_1 and the number of protons attached is roughly constant[21] supports our finding of a longer T_1 for the non-protonated carbons. At this time we have no explanation for the differences between our result and that of Gomez and Tonelli.

The quantitative calculation for the dynamic relaxation study of protonated carbon indicates that there is a large fraction of spins with longer T_1, ~ 0.94 for the as-received sample, and 0.91 for the cold crystallized sample. This leaves a fraction having much shorter T_1 of only 0.06 in the as-received sample and 0.09 in the cold crystallized sample. We believe this portion of material with much shorter T_1 comes mainly from the amorphous phase, and in particular from the most mobile amorphous chains in the semicrystalline samples. We would expect that the least mobile, RAP, along with the crystals, will have much longer relaxation times. However, the fractions deduced from the dynamic relaxation measurements (*Table 2*) are very different from the relative phase fractions deduced from thermal analysis of the glass transition (*Table 1*). The large fraction of slowly relaxing component from the dynamic n.m.r. experiment indicates that only a portion of the random-coil-like amorphous phase in the semicrystalline polymer has a short T_1. A much larger portion of random-coil-like amorphous phase has rather long T_1.

This is very consistent with the T_1 curve for purely amorphous sample, which consists of 100% liquid-like amorphous phase. The reason for the difference between thermal results and the dynamic n.m.r. results is due to the different measurement temperature. The spin-lattice relaxation measurements were done at room temperature which is far below the T_g of PPS. The very small amount of the mobile portion from the T_1 measurements indicates that at room temperature almost all material (crystal, rigid amorphous and liquid-like amorphous phases) is very rigid and relaxes very slowly. This observation is in agreement with other polymers like PEEK[22] and has been well explained by Schaefer et al.[22,23]. From the dynamic, spin-lattice relaxation measurement, we are unable to distinguish the three phases, simply because at room temperature there is no distinct difference in T_1 between the three phases. In this sense, T_1 measurements show lack of sensitivity to distinguish the heterogeneous phase behaviour at room temperature, compared with line shape or chemical shift measurements. From the standpoint of T_1, the crystals, rigid amorphous and liquid-like amorphous phases overlap and were not separable in our experiment.

One would expect that as temperature increases the portion of material with shorter T_1 obtained from the dynamic spin-lattice relaxation measurement should increase and the portion with longer T_1 should decrease. At temperatures just above T_g, the short T_1 portion determined from spin-lattice relaxation studies is expected to be comparable with the amount of liquid-like amorphous phase obtained from thermal analysis[4] or dielectric relaxation[1]. Finally, if the temperature is close to the crystal melting point the mobile portion should be close to the total fraction of amorphous phase in the semicrystalline samples[24,25]. We are now exploring the temperature dependence of the dynamic relaxation.

CONCLUSIONS

1. High resolution solid state [13]C n.m.r. has been used to study the heterogeneous phase behaviour in amorphous and semicrystalline PPS. The carbon/proton contact time dependence was studied, and the optimum contact time for cross-polarization for PPS is found to be $\sim 1000\ \mu s$.

2. Qualitatively different line widths have been found for crystal, liquid-like amorphous and rigid amorphous phases at room temperature. For as-received sample, a small amount of liquid-like amorphous was detected from ^{13}C line shape analysis and direct polarization experiments, indicating the superior sensitivity of n.m.r. over thermal analysis and dielectric relaxation analysis.

3. Spin-lattice relaxation measurements indicate that 100% amorphous PPS exhibits heterogeneous phase structure at room temperature. The longest T_1 is ~ 45 s, corresponding to mass fraction of 0.57. In semicrystalline PPS, spin-lattice relaxation measurements show a much larger amount of the material possesses longer relaxation time. The T_1 of semicrystalline PPS ranges from 150 to 200 s, corresponding to mass fractions from 0.91 to 0.94. This indicates that semicrystalline PPS is more nearly homogeneous: the crystals and most of the amorphous phase are very 'rigid' at temperatures far below the glass transition of PPS.

REFERENCES

1   Huo, P. and Cebe, P. *J. Polym. Sci., Polym. Phys. Edn* 1992, **30**, 239
2   Schlosser, E. and Schonhals, A. *Colloid Polym. Sci.* 1989, **267**, 963
3   Huo, P. and Cebe, P. *Macromolecules* 1992, **25**, 902
4   Huo, P. and Cebe, P. *Colloid Polym. Sci.* in press
5   Gaur, U. and Wunderlich, B. *J. Phys. Chem. Ref. Data* 1981, **10**, 119
6   Grebowicz, J., Lau, S. F. and Wunderlich, B. *J. Polym. Sci., Polym. Symp.* 1984, **71**, 19
7   Suzuki, H., Grebowicz, K. and Wunderlich, B. *Makromol. Chem.* 1985, **186**, 1109
8   Cheng, S., Wu, Z. and Wunderlich, B. *Macromolecules* 1987, **20**, 2802
9   Lau, S.-F. and Wunderlich, B. *J. Polym. Sci., Polym. Phys. Edn* 1984, **22**, 379
10 English, A. D. *Macromolecules* 1984, **17**, 2182
11 Nakagama, M., Horii, F. and Kitamara, R. *Polymer* 1990, **31**, 323
12 Kaji, A., Yamanaka, A. and Murana, M. *Polym. J.* 1990, **22**, 893
13 Michele, A. and Vittoria, V. *Polym. Commun.* 1991, **32**, 232
14 Chung, J. S. and Cebe, P. *J. Polym. Sci., Polym. Phys. Edn* 1992, **30**, 163
15 Chung, J. S. and Cebe, P. *Polymer* 1992, **33**, 2312
16 Chung, J. S. and Cebe, P. *Polymer* 1992, **33**, 2325
17 Torchia, D. *J. Magn. Reson.* 1978, **30**, 613
18 Clark, J., Jagannathan, N. and Herring, F. *Polym. Commun.* 1989, **30**, 212
19 Zhang, X. and Wang, Y. *Polymer* 1989, **30**, 1867
20 Gomez, M. and Tonelli, A. *Polymer* 1991, **32**, 796
21 Breitmaier, E. and Voelter, W. 'Carbon-13 NMR Spectroscopy', VCH, New York, 1987
22 Poliks, M. and Schaefer, J. *Macromolecules* 1990, **23**, 3426
23 Schaefer, J., Stejskal, E. and Buchdahl, R. *Macromolecules* 1977, **10**, 384
24 Hirschinger, J., Miura, H., Gardner, K. H. and English, A. D. *Macromolecules* 1990, **23**, 2153
25 Miura, H., Hirschinger, J. and English, A. *Macromolecules* 1990, **23**, 2169